



Universiteit
Leiden
The Netherlands

Synthesis and applications of cell wall glycopolymer fragments from Staphilococci and Enterococci

Berni, F.

Citation

Berni, F. (2023, October 19). *Synthesis and applications of cell wall glycopolymer fragments from Staphilococci and Enterococci*. Retrieved from <https://hdl.handle.net/1887/3645889>

Version: Publisher's Version

License: [Licence agreement concerning inclusion of doctoral thesis in the Institutional Repository of the University of Leiden](#)

Downloaded from: <https://hdl.handle.net/1887/3645889>

Note: To cite this publication please use the final published version (if applicable).

Chapter 5

Epitope recognition of a monoclonal antibody raised against a synthetic glycerol phosphate based teichoic acid

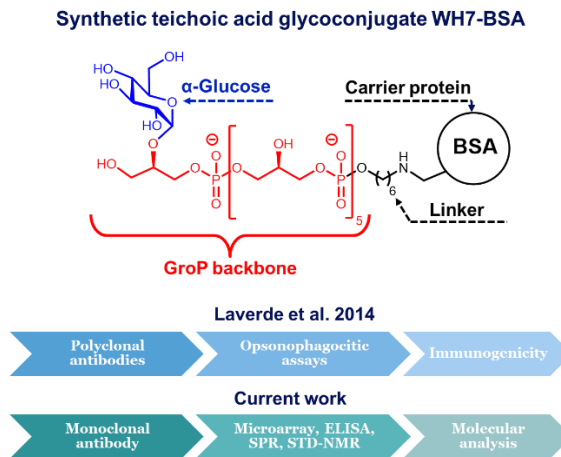
F. Berni,* E. Kalfopoulou,* A. C. Gimeno, F. Carboni, D. van der Es, F. Romero-Saavedra, D. Laverde, K. Miklic, S. Malic, T. Rovis, S. Jonjic, S. Ali, H. S. Overkleeft, C. H. Hokke, A. van Diepen, R. Adamo, J. Jiménez-Barbero, G. A. van der Marel, J. Huebner, J. D. C. Codée, *ACS Chem. Biol.*, **2021**, 16: 1344-1349.

INTRODUCTION

Teichoic acids are poly-alditolphosphate cell-wall components found in the majority of Gram-positive bacteria. They are divided into two main classes, differing in the way they are connected to the cell-wall: wall teichoic acids (WTAs) are covalently connected to the peptidoglycan, while lipoteichoic acids (LTAs) are inserted in the lipid bilayer through a lipid anchor via non-covalent, hydrophobic interactions.¹ They are involved in various biological processes and as their structure extends towards the extracellular milieu, they have been appointed as possible antigen candidates for vaccine development.²

Staphylococci and enterococci are Gram-positive bacteria, associated with a variety of severe infections.³ The prevalence of multidrug resistance strains in the clinical setting, such as methicillin-resistant *Staphylococcus aureus* (MRSA) and vancomycin-resistant enterococci (VRE), has urged the development of alternative strategies, such as active or passive immunization.⁴ LTAs from staphylococci and enterococci share a common structural motif composed of a glycerol phosphate (GroP) repeating unit.⁵ The C-2-OH of the glycerol moiety can be decorated with D-alanine or carbohydrate appendages. Previously, a synthetic TA was generated, featuring an α -glucosyl substituent at the terminal unit of a GroP hexamer (**WH7**) and conjugated to the carrier protein Bovine Serum Albumin (BSA) in order to evaluate its immunogenicity and potential as a vaccine

Figure 1: Schematic representation of the structure of the synthetic teichoic acid glycoconjugate WH7-BSA. Workflow of previous and current work.



candidate (Figure 1).⁶ It was observed that **WH7**-BSA was able to induce opsonic and protective cross-reactive antibodies against clinical isolates of *E. faecalis* **12030**, *E. faecium* E1162 and community acquired *S. aureus* MW2 (USA400), confirming the antigenic property of **WH7**. Microarray analysis showed that the polyclonal serum raised against the conjugate contained antibodies that preferentially bound α -glucosyl functionalized GroP-oligomers.⁷ Simultaneously, Snapper and co-workers used a non-

glycosylated synthetic GroP-decamer to generate a TA-conjugate and showed that this could be used to raise protective antibodies against *S. aureus*.⁸ These studies have revealed synthetic TA-fragments as attractive antigens in the generation of well-defined synthetic vaccines. The molecular basis of their immunogenicity however has not been elucidated and understanding how these fragments are recognized by the generated antibodies will provide valuable insights for the design of improved conjugate vaccines.⁹ Therefore, in the current study, the aforementioned WH7-conjugate was employed for the generation of a monoclonal antibody (WH7.01 mAb) to characterize the binding with synthetic GroP based fragments at the molecular level using TA-microarrays, ELISA, SPR-binding studies and STD-NMR. This work represents the first case-study for a synthetic GroP based TA immunogen and the detailed binding studies have revealed that all structural components, the length and chirality of the GroP backbone, as well as the presence of the carbohydrate substituent, contribute to binding of the antibody.

RESULTS AND DISCUSSION

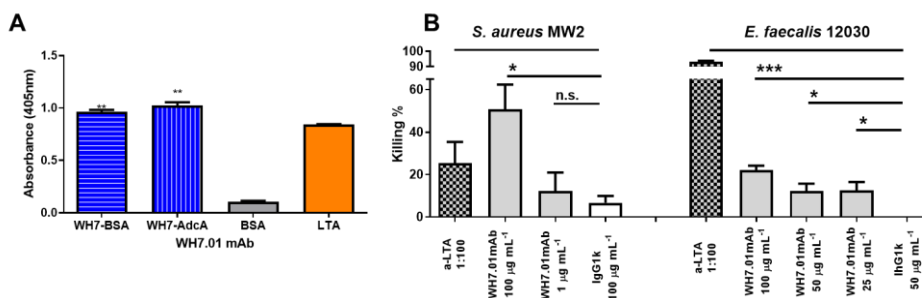
First, the hybridoma technology was implemented in order to generate a mAb against **WH7**.¹⁰ Briefly, mice were immunized with the conjugated form of **WH7** to the commonly used carrier protein BSA. The generated hybridomas were selected by ELISA against the conjugated form of **WH7** and by negative selection with BSA (see experimental section). The secreted mAb from the resulting hybridoma cell line, named WH7.01 mAb, was confirmed by ELISA to be of the IgG1 class for the heavy chain and kappa for the light chain (data not shown). WH7.01 mAb exhibited strong binding in ELISA against the **WH7**-BSA conjugate as well as towards a second conjugate that was constructed using the zinc ABC transporter substrate-binding lipoprotein AdcA¹¹ from *E. faecium* (Figure 2A). It also bound native LTAs from *S. aureus* (commercially available from Sigma) but it didn't recognize BSA neither in ELISA nor in Western blot (see experimental section). These results confirmed the development of a new mAb that specifically recognized the synthetic teichoic acid **WH7** antigen. This monoclonal was evaluated in an opsonophagocytic assay and it was observed that the WH7.01 mAb exhibited opsonic killing activity against *E. faecalis* **12030** and *S. aureus* MW2, with most killing of the latter species (Figure 2B).

Figure 2: Generation of the monoclonal antibody against WH7-BSA. A) Antigen-specificity of the supernatant from the hybridoma cell line producing the WH7.01 mAb. The binding was evaluated by ELISA against the synthetic antigen WH7 (blue) conjugated to BSA (horizontal stripes) or to AdcA (vertical stripes), the unconjugated carrier protein BSA (grey) and the commercially available LTAs from *S. aureus* (orange), all coated in duplicates with 1 µg well⁻¹. The concentration of the WH7.01 mAb in the supernatant was 35 µg mL⁻¹. Bars represent mean data and the error bars represent the standard errors of the means. Significance was inferred by two tailed unpaired t-tests between WH7 conjugates and the carrier protein (**, P<0.01). B) Opsonophagocytic killing activity of the newly generated WH7.01 mAb against *S. aureus* MW2 on the left and *E. faecalis* **12030** on the right. The opsonophagocytic killing activity of the purified monoclonal from the hybridoma cells producing WH7.01 mAb (grey) at different dilutions was evaluated against *S. aureus* MW2, and *E. faecalis* **12030**. Polyclonal sera raised in a rabbit against the purified LTA from *E. faecalis* **12030** (black and grey squares) was used as a positive control and a mAb of the same isotype, IgG1κ, was

Chapter 5

used as a negative control. Bars represent mean data and the error bars represent the standard errors of the means. n.s. (not significant), *, $P < 0.05$; ***, $P < 0.001$; all by one-way ANOVA with Dunnett's multiple comparison to the negative control (monoclonal antibody of the same isotype).

Next, the binding specificity of the newly generated monoclonal was qualitatively

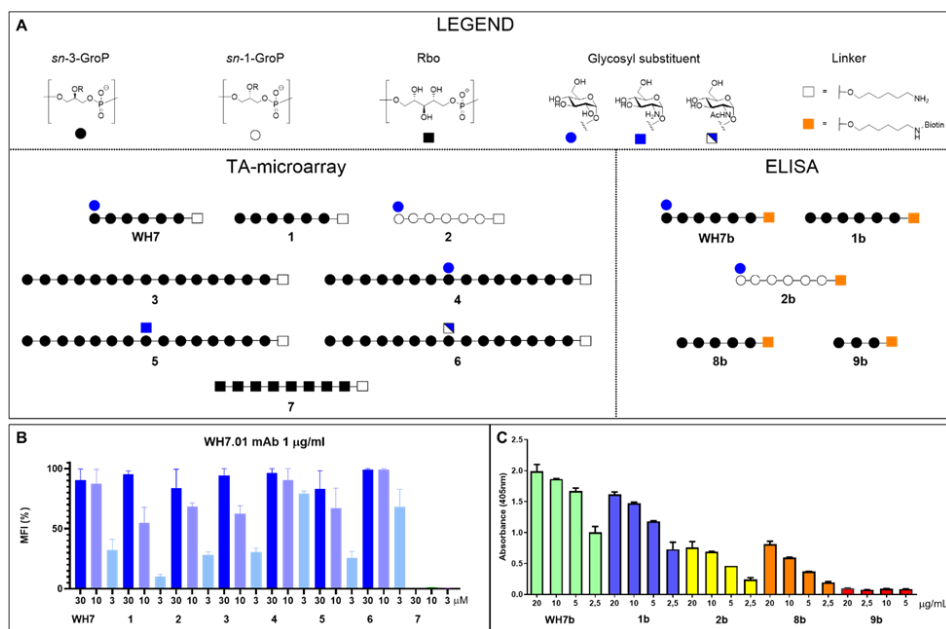


assessed using a TA-microarray. This tool allows the simultaneous screening of the binding interaction of a designated protein with a number of substrates using only minute amounts of materials.¹² In line with previous TA-microarray studies (Chapters 3 and 4),^{7,13} different synthetic GroP-fragments, each equipped with an aminohexanol linker, were covalently immobilized on an epoxide functionalized microarray glass slide. The compounds were printed on the slides in three different concentrations (30 µM, 10 µM and 3 µM) in triplicates. As shown in Figure 3A, the tested library comprises GroP-based fragments varying in length (hexamers or pentadecamers), nature of the glucosyl substituent (α -glucose, α -glucosamine or α -N-acetylglucosamine), the position of the carbohydrate on the chain (terminal or in the middle) and the stereochemistry of the glycerol unit (*sn*-1 vs. *sn*-3). Compound **7**, a ribitol phosphate chain resembling the structure of *S. aureus* WTAs,¹⁴ was included as negative control. As can be observed from the results shown in Figure 3B, the WH7.01 mAb recognized all printed GroP-based TA fragments well, indicating that the GroP-backbone is the main recognition element for the mAb. The sugar appendage also seems to contribute to binding with WH7 being recognized slightly better than its non-glucosylated counterpart **1** and α -glucosyl pentadecamer **4** showing the strongest binding among the longer GroP-fragments. The ribitol phosphate-based *S. aureus* WTA fragment **7** was not recognized by the monoclonal. To further validate the binding, ELISA assays were performed using the biotinylated derivatives **WH7b**, **1b** and **2b** as well as the shorter pentamer **8b** and trimer **9b** (Figure 3A). The synthetic fragments, tagged with biotin, were immobilized at a concentration of 1 µM on streptavidin coated plates and different dilutions of the monoclonal were employed (20 µg/ml, 10 µg/ml, 5 µg/ml, 2.5 µg/ml) in duplicates. These ELISA studies (Figure 3C) revealed that the binding of WH7.01 mAb is influenced by three structural elements: the length of the GroP chain (**1b** > **8b** >> **9b**), the presence of the glucosyl substituent (**WH7** > **1b**) and the stereochemistry¹³ of the glycerol backbone (**WH7** >> **2b**). These results overall confirm the observations from the microarray analysis, that the GroP backbone is the major structural feature that is recognized by this monoclonal antibody. At the same time, it becomes more prominent that the number of

Epitope mapping of mAb against GroP antigens

repeating units, the relative position of the C-2-OH (*sn*-1 vs *sn*-3 GroP) and the presence of the glucosyl substituent also have an impact. Previously it has been observed that the GroP backbone stereochemistry did play an important role in IgG binding of the polyclonal sera, raised against **WH7** antigen or native *E. faecalis* LTA.²³ In these cases the major epitope recognized was the glucosyl substituent, while binding of the monoclonal antibody generated here is dominated by the GroP backbone (**1b** and **8b**), likely driven by ionic interactions with the phosphate moieties. The preferential binding of the monoclonal to **WH7** compared to its diastereoisomer **2** is determined by the different GroP stereochemistry, but it also suggests a role of the glucosyl appendage to the antibody interaction. Without the glucosyl substituent, the influence of the chirality of the internal GroP residues of the *sn*-1-GroP and *sn*-3-GroP oligomers is lost.

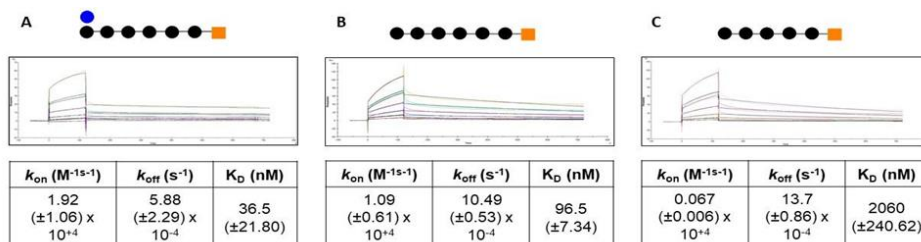
Figure 3: TA-library overview and binding assays results from microarray and ELISA. A) Overview of the synthetic fragments used for the binding analysis of WH7.01 mAb. B) TA-microarray results with WH7.01 mAb at 1 $\mu\text{g ml}^{-1}$. Compounds WH7, 1–7 were immobilized on an epoxide functionalized glass slide in three different concentrations: 30 μM (dark blue), 10 μM (shade blue) and 3 μM (light blue). The average of the triplicate spots was normalized to the highest intensity on the array. C) ELISA results of WH7.01 mAb at different concentrations against WH7b (Light green), 1b (blue), 2b (yellow), 8b (orange) and 9b (red). All biotin-derivatives were coated at the same concentration (1 μM) on a streptavidin ELISA plate. Bars represent mean data and the error bars the standard errors of the means.



In order to investigate binding in more detail, a quantitative analysis of binding parameters was performed by measuring the antibody-ligand interaction by SPR.¹⁵ To this end, **WH7b**, non-glucosylated hexamer **1b** and pentamer **8b** were immobilized on a streptavidin functionalized sensor chip. Figure 4 reveals a higher affinity towards the

hexameric fragments (**WH7b** and **1b**) than to the pentamer (**8b**). The length of the TA backbone significantly affects the k_{on} with the value for compound **8b** being 16 and 28 times lower than **1b** and **WH7b**, respectively. While **WH7b** and **1b** have the same number of GroP repeating units, the affinity slightly increases when the glucosyl substituent is present. The carbohydrate appendage contributes positively to the binding by increasing the k_{on} and decreasing the k_{off} value.

Figure 4: Binding kinetics and kinetic and affinity constants of WH7.01 mAb against WH7b (A), compound 1b (B) and 8b (C), respectively. Serial dilutions of the analyte, WH7.01 mAb (2000–62.5 nM), were run. The numbers in parentheses represent the standard deviations of k_{on} and k_{off} . Results are representative of three independent experiments.

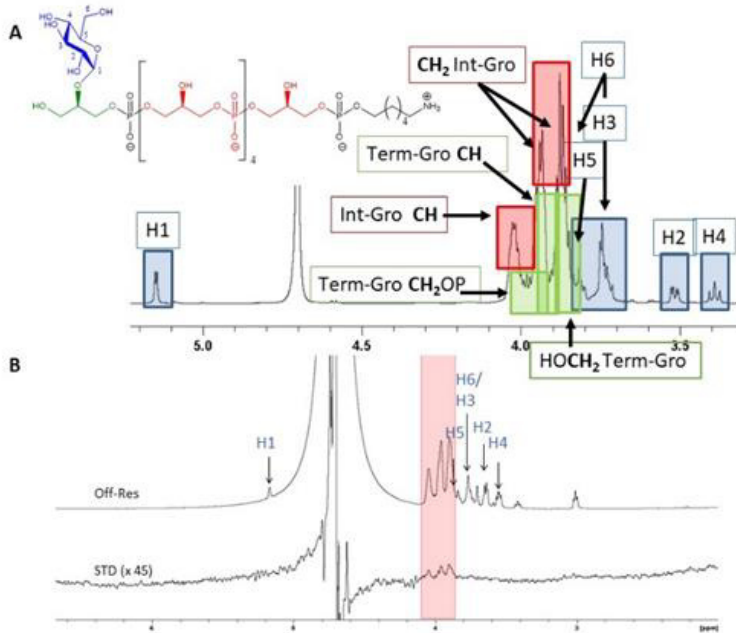


STD-NMR spectroscopy has been widely used in the last decades for structural epitope-mapping.¹⁶ Therefore, our binding study between the monoclonal and its ligand **WH7** was continued using this technique. The experiment was carried out using a 2.5 μM concentration of WH7.01 with a protein/ligand ratio of 1:100, at 303 K to avoid overlapping of the glucosyl anomeric proton with the HDO signal. Figure 5 shows the 1H -NMR spectrum of the ligand alone (A) and the STD-NMR experiment (B). Because of the repetitive nature of the ligand there is significant signal overlap of the GroP repeating units, but the signals of the glucosyl H1, H2 and H4 can be clearly distinguished. STD effects can be observed for signals related to CH/CH₂ of the glycerol units while no significant involvement of the glucosyl substituent is detected. This indicates that the sugar substituent is not directly involved in the binding of WH7.01 mAb. Taking into account the SPR results, showing that the presence of the glucosyl moiety provides a better GroP binder for the case-study antibody, it may be speculated that the glucosyl moiety reduces the conformational freedom of the terminal glycerol unit and/or provides a conformation that enables stabilizing additional contacts with the mAb, which has previously been observed in the immunorecognition of other polysaccharides.¹⁷

Figure 5: STD-NMR analysis. A) Assignment of the 1H -NMR spectrum of WH7 in D₂O at room temperature. H peaks for the intermediate GroP (Int-Gro CH/CH₂), terminal GroP (Term-Gro CH/CH₂OP/HOCH₂) and α -Glucose (H1 to 5) are assigned with red, green and blue, respectively. B)

Epitope mapping of mAb against GroP antigens

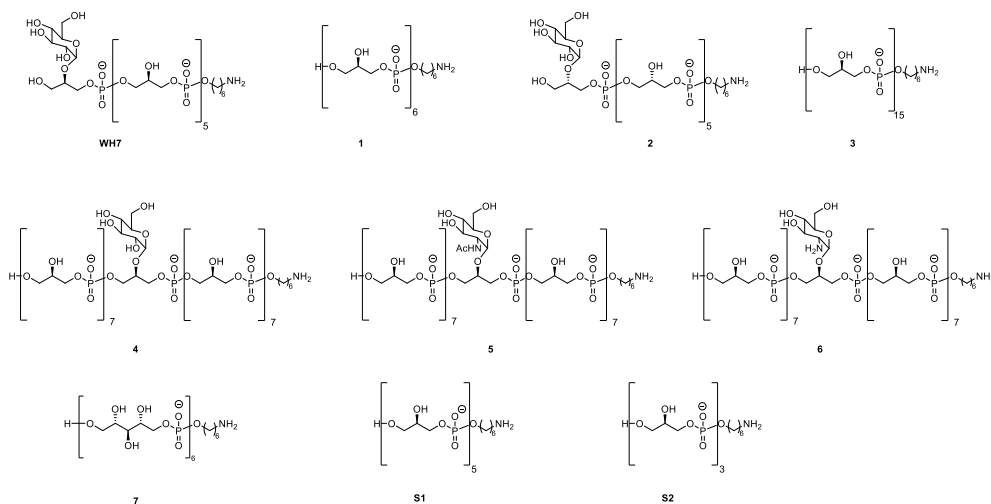
Off- (top) and on-resonance (bottom) of 1H-STD-NMR spectra between WH7.01 mAb (2.5 μ M) and WH7 (0.5 mM) at 303K.



CONCLUSION

In conclusion, the first mAb raised against a synthetic glycosylated GroP based TA has been generated by hybridoma technology. This mAb showed high binding specificity towards both the synthetic antigen and the commercially available LTA from *S. aureus*. Different techniques were used to reveal the key structural elements for ligand recognition. A first screening using a TA-microarray showed the GroP backbone as the main recognition element. Further analysis using ELISA and SPR indicated the importance of the number of GroP residues as well as a role for the glucosyl substituent. STD-NMR spectroscopy revealed interactions with the GroP backbone, but no interaction of the glucose residue with the mAb was detected. This suggests a possible indirect contribution of the glucosyl substituent to the binding. The carbohydrate may impose a particular conformational geometry to the GroP residue or backbone, leading to increased binding of the glycosylated TA. Due to the high structural heterogeneity in TAs from native sources, the availability of more well-defined TA-fragments¹⁸ can provide insights on the structural elements (the backbone, the stereochemistry, carbohydrates as well as D-Ala substituents) required for TA-antibody binding. In particular, the workflow here presented can be used in the future for the generation of a library of mAbs¹⁵ with high specificity to a variety of different poly-alditolphosphate antigen candidates and to analyze the structure-immunogenicity relationship for future TA-based vaccine development.

EXPERIMENTAL SECTION

Overview synthetic fragments**Figure 6:** Overview of the synthetic GroP-TA fragments used for the study of epitope recognition by WH7.01 mAbSynthesis of fragments WH7, 1-7, S1-S3 and WH7-BSA conjugate

The synthesis and the characterizations can be found to the corresponding references:

WH7, 1: Hogendorf, W.F.J., Meeuwenoord, N., Overkleeft, H.S., Filippov, D.V., Laverde, D., Kropec, A., Huebner, J., Van der Marel, G.A., Codée, J.D.C. (2011) Automated solid phase synthesis of teichoic acids. *Chem. Commun.* 47, 8961-8963.

3-6: Van der Es, D., Berni, F., Hogendorf, W. F. J., Meeuwenoord, N., Laverde, D., van Diepen, A., Overkleeft, H.S., Filippov, D.V., Hokke, C. H., Huebner, J., van der Marel, G. A., Codée, J. D. C. (2018) Streamlined synthesis and evaluation of teichoic acid fragments. *Chem.-Eur. J.* 24, 4014-4018.

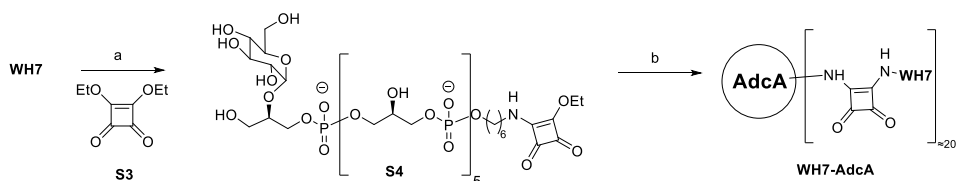
7: Hendriks, A., van Dalen, R., Ali, S., Gerlach, D., van der Marel, G. A., Fuchsberger, F. F., Aerts, P. C., de Haas, C. J. C., Peschel, A., Rademacher, C., van Strijp, J. A. G., Codée, J. D. C., van Sorge, N. M. (2021) Impact of Glycan Linkage to Staphylococcus aureus Wall Teichoic Acid on Langerin Recognition and Langerhans Cell Activation *ACS Infect. Dis.* 7, 624-635

2: Berni, F., Wang, L., Kalfopoulou, E., Nguyen, D. L., van der Es, D., Huebner, J., Overkleeft, H. S., Hokke, C. H., van der Marel, G. A., van Diepen, A., Codée, J. D. C. (2021) Generation of glucosylated sn-1-glycerolphosphate teichoic acids: glycerol stereochemistry affects synthesis and antibody interaction *RSC Chem. Biol.* 2, 187-191.

S1, S2: Hogendorf, W.F.J., Lameijer, L.N., Beenakker, T.J.M., Overkleeft, H. S., Filippov, D. V., Codée, J. D. C., Van der Marel, G. A. (2012) Fluorous linker facilitated synthesis of teichoic acid fragments. *Org. Lett.* 14, 848-851.

WH7-BSA conjugate: Laverde, D., Wobser, D., Romero-Saavedra, F., Hogendorf, W., van der Marel, G. A., Berthold, M., Kropec, A., Codee, J. D. C., Huebner, J. (2014) Synthetic Teichoic Acid Conjugate Vaccine against Nosocomial Gram-Positive Bacteria. *PLoS ONE.* 9(10): e110953.

Generation of WH7-AdcA conjugate



Scheme 1: Generation of WH7-AdcA conjugate. a) S3, PBS (pH=8), EtOH, 92%; b) S4, borate buffer (pH=9).

WH7-ethylsuarate (S4)

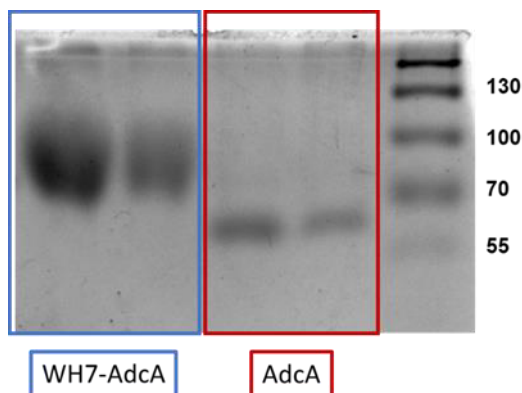
Hexamer **WH7** (10 mg, 8.3 μmol) was dissolved in a mixture of water (0.83 ml) and sodium phosphate buffer (1 M, pH=8, 42 μl). A solution of 3,4-Diethoxy-3-cyclobutene-1,2-dione (S3, 0.04 M in EtOH, 1.0 ml, 42 μmol) was added. The mixture was stirred for 24 hours and the EtOH was evaporated by flushing dry air over the reaction mixture. The mixture was purified by size-exclusion chromatography (HW40, dimensions: 16/60 mm, eluent: 0.15 M NH_4OAc). After repeated lyophilization, the product was eluted through a small column containing Dowex Na^+ cation-exchange resin (type: 50WX4-200, stored on 0.5 M NaOH in H_2O , flushed with H_2O and MeOH before use). Lyophilization gave squarate equipped hexamer S4 (10.2 mg, 7.7 μmol) in 92% yield. ^1H NMR (500 MHz, D_2O) δ : 5.18 (d, $J = 3.9$ Hz, 1H), 4.12 – 4.02 (m, 6H), 4.01 – 3.95 (m, 10H), 3.94 – 3.82 (m, 16H), 3.82 – 3.72 (m, 4H), 3.69 – 3.58 (m, 1H), 3.58 – 3.48 (m, 2H), 3.42 (t, $J = 9.7$ Hz, 1H), 3.35 (s, 2H), 1.93 (s, 6H), 1.71 – 1.59 (m, 4H), 1.50 – 1.37 (m, 7H); ^{31}P NMR (202 MHz, D_2O) δ 1.5, 1.4, 1.4.

WH7-AdcA conjugate

AdcA was overexpressed and purified as described previously.¹ Squarate **S4** (1.6 mg, 1.3 μmol) was dissolved in borate buffer (0.5 M, pH=9.0, 100 μl) and transferred to a vial containing AdcAFM (2.8 mg, 0.05 μmol) in PBS (20 μl). The mixture was shaken for 16 hours and passed over a Micro Bio-Spin Column (Bio-Gel P-6, Bio-Rad, pretreated with PBS) yielding WH7-AdcA conjugate. SDS-PAGE was used to check the formation and purification of the conjugate, while with orcinol mediated glycoside quantification a loading of ~ 20 hexamers per protein was observed.

Chapter 5

Figure 7: SDS-PAGE on WH7-AdcA conjugate (blue) and AdcA (red)



General procedure for orcinol mediated glycoside quantification

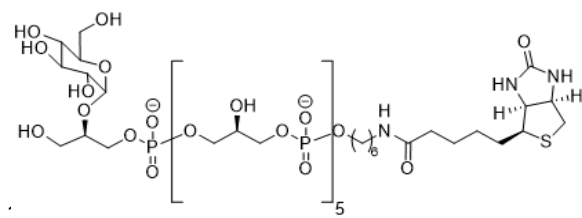
A series of defined glucose solutions (0.1, 0.2, 0.4, 0.6, 0.8 and 1 mg ml⁻¹) was prepared. The solutions (100 μ l) were gently mixed with a solution of orcinol (20 mg ml⁻¹ in 25% H₂SO₄, 200 μ l) in glass vials. H₂SO₄ (60%, 1.5 ml) was added forcefully and the mixtures were heated for 20 minutes at 80°C. The absorbance at 530 nm was measured for all samples and a calibration trend line was constructed. The conjugate was diluted to two concentrations (25 μ M and 30 μ M) and both dilutions (100 μ l) were treated as described above. The absorbance at 530 nm was measured for both dilutions and they were plotted on the trend line to reveal the glucose concentration. Combined with the protein concentration, based on the initial protein concentration, loading was determined.

Synthesis of biotinylated fragments

General procedure

The synthetic fragment was dissolved in DMSO (2 mM), then DIPEA (1.5 eq) and Biotin-OSu (1.3 eq) were added and the mixture stirred overnight at room temperature. After centrifugation, the biotinylated fragment was purified by size exclusion chromatography (HW-40 column, dimensions: 16/60 mm, eluent 0.15 M NH₄OAc). After repeated co-evaporation with milliQ water to remove NH₄OAc, the product was eluted through a small column containing Dowex Na⁺ cation-exchange resin (type 50WX8-50-100, stored on 0.5 M NaOH in H₂O, flushed with H₂O and MeOH before use). Lyophilization yielded the product, which was characterized by ¹H-NMR.

Compound WH7b

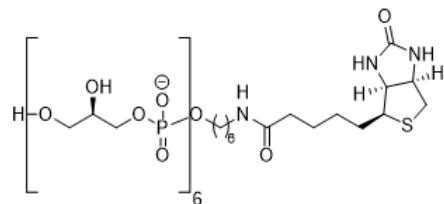


Starting from **WH7** (1 mg, 0.8 μ mol), following the general procedure, compound **WH7b** (0.83 mg, 0.5 μ mol) was isolated in 65% yield.

Epitope mapping of mAb against GroP antigens

^1H NMR (500 MHz, D_2O) δ : 5.14 (d, $J=3.9$ Hz, 1H), 4.61–4.54 (m, 1H), 4.44–4.36 (m, 1H), 4.07–3.66 (m, 36H), 3.55–3.47 (m, 1H), 3.43–3.26 (m, 2H), 3.20–3.09 (m, 3H), 3.02–2.93 (m, 1H), 2.75 (d, $J=12.0$ Hz, 1H), 2.28–2.17 (m, 2H), 1.79–1.26 (m, 14H)

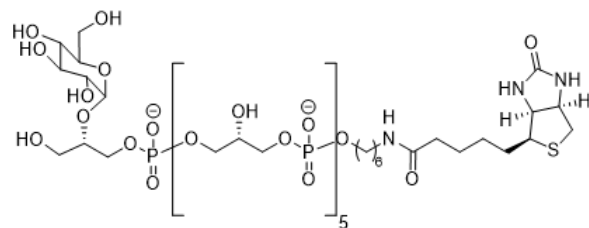
Compound 1b



Starting from **1** (2.7 mg, 2.6 μmol), following the general procedure, compound **1b** (2.3 mg, 1.6 μmol) was isolated in 61% yield.

^1H NMR (500 MHz, D_2O) δ : 4.61–4.52 (m, 1H), 4.44–4.33 (m, 1H), 4.07–3.71 (m, 28H), 3.69–3.61 (m, 1H), 3.60–3.50 (m, 1H), 3.34–3.26 (m, 1H), 3.20–3.06 (m, 2H), 3.00–2.91 (m, 1H), 2.75 (d, $J=12.0$ Hz, 1H), 2.27–2.16 (m, 2H), 1.78–1.23 (m, 14H)

Compound 2b

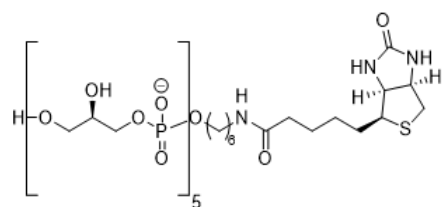


Starting from **2** (2.7 mg, 0.5 μmol), following the general procedure, compound **2b** (0.6 mg, 0.4 μmol) was isolated in 80% yield.

^1H NMR (500 MHz, D_2O) δ : 5.15 (d, $J=3.9$ Hz, 1H), 4.61–4.54 (m, 1H), 4.44–4.36 (m, 1H), 4.14–3.79 (m, 30H), 3.79–3.69 (m, 2H), 3.69–3.61 (m, 1H),

3.61–3.52 (m, 1H), 3.52–3.45 (m, 1H), 3.41–3.28 (m, 2H), 3.21–3.09 (m, 3H), 3.01–2.93 (m, 1H), 2.75 (d, $J=12.0$ Hz, 1H), 2.28–2.17 (m, 2H), 1.80–1.24 (m, 14H)

Compound 8b

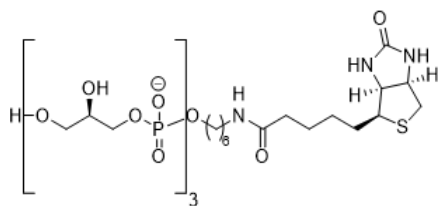


Starting from **S1** (0.49 mg, 0.6 μmol), following the general procedure, compound **8b** (0.3 mg, 0.2 μmol) was isolated in 33% yield.

^1H NMR (500 MHz, D_2O) δ : 4.61–4.52 (m, 1H), 4.44–4.33 (m, 1H), 4.07–3.71 (m, 25H), 3.69–3.61 (m, 1H), 3.60–3.50 (m, 1H), 3.34–3.26 (m, 1H), 3.20–3.06 (m, 2H), 3.00–2.91 (m, 1H), 2.75 (d, $J=12.0$ Hz, 1H),

2.27–2.16 (m, 2H), 1.78–1.23 (m, 14H)

Compound 9b



Starting from **S2** (0.8 mg, 1.4 μmol), following the general procedure, compound **9b** (0.6 mg, 0.7 μmol) was isolated in 50% yield.

^1H NMR (500 MHz, D_2O) δ : 4.61–4.52 (m, 1H), 4.44–4.33 (m, 1H), 4.07–3.71 (m, 15H), 3.69–3.61 (m, 1H), 3.60–3.50 (m, 1H), 3.34–3.26 (m, 1H), 3.20–3.06 (m, 2H), 3.00–2.91 (m, 1H), 2.75 (d, $J=12.0$ Hz, 1H),

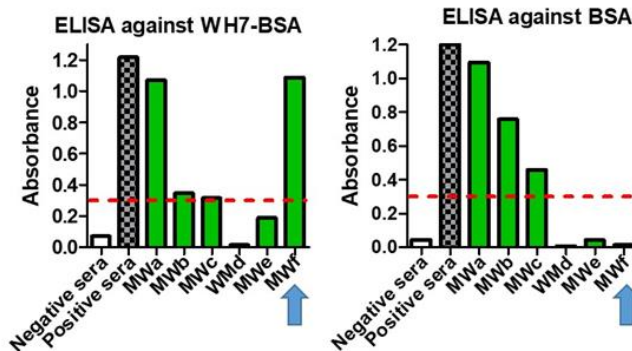
2.27–2.16 (m, 2H), 1.78–1.23 (m, 14H)

Generation of the mouse monoclonal antibody

Three BALB/c mice were immunized by two subcutaneous injections of 50 μg , in protein content, of the glycoconjugate **WH7**-BSA with Freund's incomplete adjuvant given 2 weeks apart. The mouse sera were screened by ELISA for antibody titers against **WH7**-BSA and three weeks later, mice were subjected to a final intraperitoneal injection of 50 μg of glycoconjugate in PBS. Three days after the injection, mice were sacrificed and the splenocytes were isolated, red blood cells were eliminated by lysis and fusion of the splenocytes with SP2/O myeloma cells was performed at a 1:1 ratio. The cells were resuspended in RPMI supplemented with 20% fetal bovine serum (FBS) (PAN-Biotech) and hypoxanthine, aminopterin, and thymidine (Gibco) for the selection of the hybridomas and were equally distributed into six 96-well plates. The supernatants from the mother-wells (MWs) were selected by ELISA against **WH7**-BSA and by negative selection with ELISA against BSA. At the first selection point, from the three independent fusions, 1800 MWs were obtained and screened. From these MWs, only six were considered positive, having an absorbance of over 0.3 in ELISA against **WH7**-BSA. These six MWs were retested and the final screening is represented in Figure 3. The mother-well MWf that exhibited immune specificity to WH7 (Figure 3) was subjected to cloning by limiting dilution to obtain monoclonal cell populations. The obtained cell line was propagated and maintained in 10% FBS, 2 mM l-glutamine, 25 mM HEPES, and RPMI 1640 (Gibco). For the purification of the monoclonal antibody, the hybridoma cells were seeded in Nunclon Delta surface three layer flasks (Thermo scientific) and grown in ISF-1 medium (Biochrom). After one week the supernatants were collected and purified using Protein G Gravitrapp purification columns (GE Healthcare) according to manufacturers' instructions. The elution buffer was exchanged to PBS for the antibody storage using 10kDa molecular weight cutoff Amicon Ultra centrifugal filters (Millipore).

Epitope mapping of mAb against GroP antigens

Figure 8: Final selection of the immunoreactive hybridoma mother wells by ELISA screening against WH7-BSA conjugate and BSA. The supernatants from the mother-wells are indicated with MWa to f. Mouse sera before and after immunization with WH7 were used at 1:1000 ratio as a negative (white) and positive control (black and grey squares), respectively. The mother well with immunospecificity to WH7 is indicated with a blue arrow. Absorbance of 0.3, indicated here with a red dashed line, is used as a threshold for positive signal.



Quantification of mouse IgG concentrations

The concentration of the purified mAbs and the rabbit sera were determined by sandwich ELISA as previously described by Salauze et al.³ Nunc-immuno Maxisorp MicroWell 96 well plates were coated with 0.1 μg per well of unlabeled a-mouse IgG antibody (SouthernBiotech) or a-rabbit IgG antibody (Sigma-Aldrich) in 0.2 M carbonate-bicarbonate. After an overnight incubation at 4°C, wells were washed three times with 200 μL washing buffer (0.9% sodium chloride, 0.1% Tween 20) and incubated with the same volume of blocking buffer (3% BSA in PBS) for 2 hours at RT. After blocking, wells were washed three times with 200 μL washing buffer and 100 μL of serial dilutions in blocking buffer of either the purified mAbs or the rabbit sera were plated in triplicate. In addition, 100 μL of dilutions in blocking buffer of either standard mouse IgG (SouthernBiotech) or rabbit IgG ranging from 31.2 ng mL^{-1} to 0.24 ng mL^{-1} were plated in triplicates. After 2 hours incubation, wells were washed three times with 200 μL washing buffer and 100 μL of the secondary antibody, AP conjugated a-mouse or a-rabbit IgG produced in goat (Sigma-Aldrich), at 1:1000 dilution were added. The incubation was carried out for 2 hours at RT, the wells were washed four times with washing buffer and detection was performed using 100 μL of p-nitrophenyl phosphate at 1 mg mL^{-1} in glycine buffer. After 30 min of incubation at RT in the dark, the absorbance was measured at 405 nm. For the calculation of the antibody concentration the calibration curves of the standard mouse or rabbit IgG dilutions were used.

Bacterial Strains and Rabbit Immunizations

The bacterial strains used in this study were the clinical strain *E. faecalis* 12030,4 and the community-acquired *S. aureus* MW2 (USA 400).⁵ All strains were grown in tryptic soy

Chapter 5

agar and broth (Carl Roth) at 37°C with and without agitation, for *S. aureus* MW2 and *E. faecalis* 12030, respectively. a-LTA serum was obtained upon immunization of a New Zealand white rabbit with purified LTA from *E. faecalis* 12030 as described elsewhere.⁶

ELISA against WH7 conjugates and LTA from *S. aureus*

Nunc-immuno Maxisorp MicroWell 96 well plates were coated with 1 µg per well of BSA, **WH7**-BSA, **WH7**-AdcA and lipoteichoic acid from *Staphylococcus aureus* (Sigma) in 0.2 M carbonate-bicarbonate (15 mM sodium carbonate, 35 mM sodium bicarbonate, pH=9.6) and incubated overnight at 4°C. The next day the plates were washed three times with 200 µL washing buffer (PBS, 0.05% Tween 20) and blocked with 3% BSA in PBS for 1 hour at 37°C. After blocking, plates were washed two times with 200 µL washing buffer and 100 µL of the serial dilutions of the supernatants from the hybridomas or the immune rabbit sera in blocking buffer (3% BSA in PBS) were plated in triplicate. After 1 hour incubation, the plates were washed three times with 200 µL washing buffer and 100 µL of the secondary antibody, alkaline-phosphatase-conjugated (AP conjugated) a-mouse or a-rabbit IgG produced in goat (Sigma-Aldrich), at 1:1000 dilution was added. The plates were incubated for 1 hour at room temperature (RT), washed three times with washing buffer and the detection was performed using 100 µL of p-nitrophenyl phosphate (Sigma-Aldrich) at 1 mg mL⁻¹ in glycine buffer (0.1 M glycine, 1 mM MgCl₂, 1 mM ZnCl₂, pH=10.4). After 30 min of incubation at RT in the dark, absorbance was measured at 405 nm in an ELISA reader (Synergy H1 Hybrid reader, BioTek, USA). For the selection of the clones and the determination of the isotype ELISA was performed as described previously.⁷

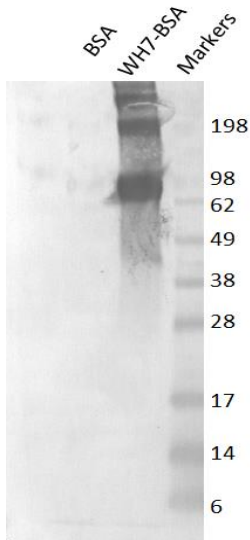
Western blotting

BSA and conjugated BSA with **WH7** (**WH7**-BSA) were analyzed by SDS-PAGE and subsequently by western blotting as described before.⁷ After western blotting the membrane was blocked with blocking buffer (BB; 3% bovine serum albumin in PBS) overnight at 4°C. The next day, it was washed three times with washing buffer (WB; PBS, 0.05% Tween 20) and incubated for 1 hour with supernatant from the hybridoma cell line expressing WH7.01 mAb at 8.99 µg ml⁻¹. The membrane was then washed again as described above and incubated for 1 hour with alkaline phosphatase-conjugated anti-mouse IgG (Sigma-Aldrich) diluted 1:1000 in BB. Finally, three washes with WB were performed and binding was detected by the colorimetric AP substrate reagent kit (Bio-Rad).

Figure 9: Western blotting against **WH7**-BSA conjugate (right) and carrier protein BSA (left) using the supernatant from hybridoma expressing WH7.01 mAb. SeeBlue Plus2 prestained protein

Epitope mapping of mAb against GroP antigens

standard (Markers) was used to assess the molecular weight of the samples, e.g., **WH7-BSA** is around 98 kDa as reported before.⁸



Opsonophagocytic assay (OPA)

MAb activity was evaluated by OPA as previously described⁹ using the bacterial strain, baby complement, white blood cells (WBCs) and purified mAb without antibiotics. Polyclonal rabbit sera raised against native LTA from *E. faecalis* **12030** was used as positive control while IgG1k mAb, a monoclonal of the same isotype as WH7.01 mAb, was used as negative control. Bacteria were grown at 37°C until the optical density at 650 nm reached 0.4 and adjusted to a final concentration of 2×10^7 CFU ml⁻¹ in RPMI 1640 (Gibco) with 15% FBS (termed 15% RPMI). Rabbit complement (Cedarlane) was diluted at a final concentration of 6.7%, vol/vol, in 15% RPMI, incubated with the target strain for 60 min at 4°C with shaking, and filter sterilized. WBCs, freshly isolated from a healthy human donor, were prepared by mixing blood with an equal volume of heparin-dextran buffer. After incubation for 45 min at 37°C, the upper layer was collected and centrifuged (at 2.700 rpm for 10 min at 10°C) and the resulting pellet was washed with 15% RPMI. The erythrocytes in the pellet were lysed with 1% NH₄Cl (Sigma-Aldrich) at RT for 20 min. WBCs were washed again and resuspended in 15% RPMI to yield a final concentration of $\approx 2 \times 10^7$ cells ml⁻¹. The four components were added in equal volumes and incubated on a rotor rack at 37°C for 90 min. The samples were plated in quadruplicates to enumerate the CFU. The percentage of killing was calculated by comparing the surviving CFU in the reaction WBCs (WBCpos) to the surviving CFU in the tubes lacking WBCs (WBCneg) using the following formula: % killing = $100 - [100 \times (\text{WBCpos mean CFU at 90 min}) / (\text{WBCneg mean CFU at 90 min})]$. Negative controls lacking one, two or three of the components were included in the assay. In all experiments presented, no killing was observed for these four negative controls.

Microarray analysis

The amino-spacer equipped synthetic fragments (**WH7**, 1–7) were dissolved in spotting buffer (Nexterion Spot, Schott Nexterion) with 10% DMSO in 384-wells V-bottom plates (Genetix, New Milton, UK). The fragments were printed in three final concentrations (30 μM , 10 μM and 3 μM) in triplicate on epoxysilane-coated glass slides (Slide E, Schott, Nexterion) by contact printing using the Omnigrid 100 microarrayer (Genomic Solutions, Ann Arbor, MI) equipped with SMP3 pins with uptake channels that deposit 0.7 nl at each contact. The slides were rested in a high humidity chamber for 18 hours and were stored in the dark until used. The slides were washed with PBS (3x) and subsequently all unreacted sites on the arrays were blocked by shaking the slides for 1 hour with ethanolamine (0.10 ml, 0.05 M in PBS containing 20 mg ml^{-1} of BSA). The slides were flushed with PBS containing 5% of Tween[®] 20 and then PBS and finally rinsed with PBS containing 1% of Tween[®] 20. After removal of the PBS containing 1% of Tween[®] 20, the arrays were shaken with WH7.01 mAb at 1 $\mu\text{g ml}^{-1}$ (0.10ml, diluted with PBS containing 1% of Tween[®] 20 and 10 mg ml^{-1} of BSA) for 60 minutes. The slides were flushed with PBS containing 5% of Tween[®] 20 and PBS and rinsed with PBS containing 1% of Tween[®] 20 subsequently. After removal of the PBS containing 1% of Tween[®] 20, the arrays that were goat anti-mouse IgG (H+L) secondary antibody, Alexa Fluor[®] 555 conjugate (Invitrogen, A21422), (0.10 ml, 0.5 $\mu\text{g ml}^{-1}$ final dilution in PBS containing 1% of Tween[®] 20 and 10 mg ml^{-1} of BSA) for 30 minutes in the dark. The slides were flushed with PBS containing 5% of Tween[®] 20, PBS and MilliQ subsequently. The slides were dried by centrifugation and were analyzed on fluorescence on 532 nm and 635 nm using a G2565BA scanner. Data and image analyses were performed with GenePix Pro 7.0 software (Molecular Devices, Sunnyvale, CA, USA) as described previously. 10 Fluorescence intensities were quantified and corrected for background/non-specific antibody adhesion by subtracting the fluorescence at blank spots, where spotting buffer was printed without GTA fragment. The average of the triplicate spots was normalized to the highest intensity on the array and visualized in bar graphs using GraphPad Prism 8.4.3.

ELISA against the synthetic fragments

The monoclonal antibody specificity to the synthetic teichoic acid fragments was evaluated by ELISA. Streptavidin coated plates (Thermo Scientific Pierce) were washed three times with 200 μL wash buffer (WB: 25 mM Tris, 150 mM NaCl, 0.1% BSA and 0.05% Tween 20, adjusted to pH=7.2). The wells were coated in duplicate with 1.0 μM of the synthetic teichoic acid fragments dissolved in WB. After 2 hours of incubation at 4°C, the plates were washed three times with 200 μL WB and incubated with 100 μL of WH7.01 mAb at the specified concentrations for 2 hours at RT with gentle shaking. Wells were washed three times with 200 μL WB and incubated for 30 min with gentle shaking at RT with 100 μL of alkaline-phosphatase-conjugated anti-mouse IgG produced in goat (Sigma, St. Louis, Mo.) at 1:1000 dilution in WB. After three washes with 200 μL of WB, the detection was performed with 100 μL of p-nitrophenyl phosphate (Sigma-Aldrich) at 1 mg ml^{-1} in glycine buffer. After 10 min of incubation at RT in the dark, the reaction was

stopped with 50 μ L of 3 M sodium hydroxide and the absorbance was measured at 405 nm in a Synergy H1 hybrid reader (BioTek).

Surface plasmon resonance

Binding kinetics and affinities were determined by SPR using a Biacore X100 system as described elsewhere.¹¹ In order to achieve a 1:1 binding model, immobilizations of the biotinylated synthetic compounds were performed on high-affinity streptavidin (SA) sensor chips (GE Healthcare) starting from low amounts of the biotinylated compounds in water (0.1 nM) and increasing until a detectable interaction with the mAb was reported at 100 nM of the compound in water. Serial dilutions of the analyte, WH7.01 mAb (2000 – 62.5 nM), were run. Sensorgram data were analyzed using BIAevaluation software (Biacore).

1H-STD-NMR

STD experiment was acquired using Bruker AVANCE 2 600 MHz spectrometer equipped with cryoprobe. The samples were prepared in deuterated phosphate-buffered saline (10 mM sodium phosphate, 137 mM NaCl, 2.7 mM KCl, pH=7.4). WH7.01 mAb was exchanged in the working buffer using 10kDa molecular weight cutoff Amicon Ultra centrifugal filters (Millipore). After several washing the antibody concentration was determined by absorbance ($\epsilon=120500 \text{ M}^{-1}\text{cm}^{-1}$). The sample for the STD experiment was prepared using a mAb/ligand ratio of 1:100 with mAb concentration of 2.5 μ M in a shigemi 5 mm NMR microtube. In order to avoid overlapping of the glucosyl anomeric proton with the H₂O signal, the temperature was set at 303 K. The on-resonance was tested both in the aromatic and aliphatic region but no difference in STD effects was observed. Moreover, a negative control spectrum was performed in the absence of the monoclonal antibody to ensure the interpretation of the result. Finally, the on-resonance frequency was set at 0.17 ppm, while the off-resonance frequency at 100 ppm. Protein saturation was achieved by using a train of 50 ms Gaussian-shaped pulses with a total saturation time of the protein of 2s and a spin-lock filter (10 ms) was used to remove the NMR signals of the macromolecule.

Ethics statement.

Mouse experiments were approved by the Ethics Committee of the Veterinary Department of the Ministry of Agriculture and Animal Welfare Committee of the University of Rijeka, Faculty of Medicine. This study was carried out in accordance with the recommendations of regulations on the protection of animals used for scientific purposes (Official Gazette of the Republic of Croatia, 55/2013).

Chapter 5

References

- ¹ a) F. C. Neuhaus, J. Baddiley; *Mol. Biol. Rev.*, **2003**, 67: 686-723; b) S. Brown, J. P. Santa Maria, S. Walker; *Annu. Rev. Microbiol.*, **2013**, 67: 313-336; c) M. G. Percy, A. Gründling; *Annu. Rev. Microbiol.*, 2014, **68**, 81-100; O. Schneewind, D. Missiakas D.; *J. Bacteriol.*, **2014**, 196: 1133-1142.
- ² a) C. Weidenmaier, A. Peschel; *Nat. Rev. Microbiol.*, **2008**, 6: 276-287. b) C. Rockel, T. Hartung; *Release Front. Pharmacol.*, **2012**, 3: 1-19. c) D. J. Jung, J.-H. An, K. Kurokawa, Y.C. Jung, M.J. Kim, Y. Aoyagi, M. Matsushita, S. Takahashi, H.S. Lee, K. Takahashi, B. L. Lee; *J. Immunol.*, **2012**, 189: 4951.
- ³ (a) H. J. Monstein, M. Quednau, A. Samuelsson, S. Ahrne, B. Isaksson, J. Jonasson; *Microbiol.*, **1998**, 144: 1171-1179. b) R. van Dalen, A. Peschel, N. M. van Sorge, *Trends Microbiol.*, **2020**, 28: 869.
- ⁴ a) A. M. Guzman Prieto, W. van Schaik, M. R. C. Rogers, T. M. Coque, F. Baquero, J. Corander, R. J. L. Willems; *Front Microbiol.*, **2016**, 7:788. b) D. M. Livermore, *Int. J. Antimicrob. Agents*, **2000**, 16: S3-10. c) A. Zapun, C. Contreras-Martel, T. Vernet, *FEMS Microbiol Rev.*, **2008**, 32:361-85.
- ⁵ a) W. Fischer; *Adv. Microbil Phys.*, **1988**, 29: 233-302. b) S. Kodali, E. Vinogradov, F. Lin, N. Khoury, L. Hao, V. Pavliak, C. H. Jones, D. Laverde, J. Huebner, K. U. Jansen, A. S. Anderson, R. G. K. Donald; *J. Biol. Chem*, **2015**, 290: 19512. c) A. R. Sanderson, J. L. Strominger, S. G. Nathenson, R. J. Sanderson; *Biol. Chem.*, **1962**, 237: 3603. d) W. Fischer; *New Comp. Biochem.*, **1994**, 27: 199-215.
- ⁶ D. Laverde, D. Wobser, F. Romero-Saavedra, W. Hogendorf, G.A. van der Marel, M. Berthold, A. Kropec, J. D. C. Codée, J. Huebner; *PloS One.*, **2014**, 9: e110953.
- ⁷ D. van der Es, F. Berni, W. F. J. Hogendorf, N. Meeuwenoord, D. Laverde, A. van Diepen, H. S. Overkleeft, D. V. Filippov, C. H. Hokke, J. Huebner, G. A. van der Marel, J. D. C. Codée, *Chem. Eur. J.*, **2018**, 24: 4014-4018.
- ⁸ Q. Chen, J. Dintaman, A. Lees, G. Sen, D. Schwartz, M. E. Shirtliff, S. Park, J.C. Lee, J. J. Mond, C. M. Snapper; *Infect. Immun.*, **2013**, 81: 2554-2561.
- ⁹ a) C. Anish, B. Schumann, C. L. Pereira, P. H. Seeberger; *Chem Biol*, **2014**, 21:38-50. b) M. A. Oberli, M. Tamborrini, Y. H. Tsai, D. B. Werz, T. Horlacher, A. Adibekian, D. Gauss, H. M. Möller, G. Pluschke, P. H. Seeberger; *J. Am. Chem. Soc.*, **2010**, 132: 10239-10241. c) C. E. Martin, F. Broecker, M. A. Oberli, J. Komor, J. Mattner, C. Anish, P. H. Seeberger; *J. Am. Chem. Soc.*, **2013**, 135: 9713-9722. d) B. Schumann, C. L. Pereira, P. H. Seeberger;

Chem. Biol., **2014**, 21:38–50. e) F. Broecker, C. Anish, P. H. Seeberger; *Methods Mol. Biol.*, **2015**, 1331:57-80.

¹⁰ a) A.K. Varshney, X. Wang, J. MacIntyre, R.S. Zollner, K. Kelleher, O. V. Kovalenko, X. Pechuan, F. R. Byrne, B. C. Fries; *J. Infect. Dis.*, **2014**, 210:973–981. b) T. B. Nielsen, P. Pantapalangkoor, B. M. Luna, K. W. Bruhn, J. Yan, K. Dekitani, S. Hsieh, B. Yeshoua, B. Pascual, E. Vinogradov, K. M. Hujer, T. N. Domitrovic, R. A. Bonomo, T. A. Russo, M. Leszczyniecka, T. Schneider, B. Spellberg; *J. Infect. Dis.*, **2017**, 216:489–501. c) E. Diago-Navarro, M. P. Motley, G. Ruiz-Peréz, W. Yu, J. Austin, B. M. Seco, G. Xiao, A. Chikhalya, P.H. Seeberger, B.C. Fries; *mBio*, **2018**, 9:e00091-18. d) L. M. Guachalla, K. Hartl, C. Varga, L. Stulik, I. Mirkina, S. Malafa, E. Nagy, G. Nagy, V. Szijártó, *Antimicrob. Agents Chemother.*, **2017**, 61:e01428-17. e) S. Rohatgi, D. Dutta, S. Tahir, D. Sehgal; *J. Immunol.*, **2009**, 182:5570 –5585.

¹¹ F. Romero-Saavedra, D. Laverde, A. Budin-Verneuil, C. Muller, B. Bernay, A. Benachour, A. Hartke, J. Huebner; *PLoS One*, **2015**, 10:e0136625.

¹² S. Park, J. C. Gildersleeve, O. Blixt, I. Shin; *Chem. Soc. Rev.*, **2013**, 42: 4310.

¹³ F. Berni, L. Wang, E. Kalfopoulou, D.L. Nguyen, D. van der Es, J. Huebner, H. S. Overkleeft, C. H. Hokke, G. A. van der Marel, A. van Diepen, J. D. C. Codée; *RSC Chem. Biol.*, **2021**, 2: 187-191.

¹⁴ A. Hendriks, R. van Dalen, S. Ali, D. Gerlach, G. A. van der Marel, F. F. Fuchsberger, P. C. Aerts, C. J. C. de Haas, A. Peschel, C. Rademacher, J. A. G. van Strijp, J. D. C. Codée, N. M. van Sorge; *ACS Infect. Dis.*, **2021**, 7,:624-635.

¹⁵ G. Safina; *Anal. Chim. Acta.*, **2012**, 712: 9-29.

¹⁶ A. Ardà, J. Jiménez-Barbero; *Chem. Commun.*, **2018**, 54: 4761-4769.

¹⁷ a) J. M. Fox, M. Zhao, M.J. Fink, K. Kang, G. M. Whitesides; *Annu. Rev. Biophys.*, **2018**, 47:223–50. b) A. Gimeno, S. Delgado, P. Valverde, S. Bertuzzi, M.A. Berbis, J. Echavarren, A. Lacetera, S. Martín-Santamaría, A. Suroliá, F.J. Cañada, J. Jiménez-Barbero, A. Ardà; *Angew. Chem. Int. Ed.*, **2019**, 58:7268-7272. c) P. Henriques, L. Dello Iacono, A. Gimeno, A. Biolchib, M. R. Romano, A. Ardà, G. J. L. Bernardes, J. J. Barbero, F. Berti, R. Rappuoli, R. Adamo; *Proc. Nat. Acad. Sci. USA*, **2020**, 117: 29795–29802.

¹⁸ S. Ali, A. Hendriks, R. van Dalen, T. Bruyning, N. Meeuwenoord, H. S. Overkleeft, D. Filippov, D., G. A. van der Marel, N.M. van Sorge, J. D. C. Codée; *Chem.-Eur. J.*, **2021**, 27: 10461-10469.